EUROPEAN ORGANIZATION FOR NUCLEAR RESEARCH

CERN-EP/85-194
26 November 1985

SEARCH FOR A ϕ' VECTOR MESON IN DIFFRACTIVE PHOTOPRODUCTION OF $K^+K^-\pi^+\pi^-$

Bonn[1]-CERN[2]-Glasgow[3]-Lancaster[4]-Manchester[5]-Paris VI[6]
-Rutherford[7]-Sheffield[8] collaboration

(The Omega Photon Collaboration)

M. Atkinson[7], T. J. Axon[5], D. Barberis[5], T. J. Brodbeck[4],
G. R. Brookes[8], J. J. Bunn[8], P. J. Bussey[3], A. B. Clegg[4],
J. B. Dainton[3], M. Davenport[7], B. Dickinson[5], B. Diekmann[1],
A. Donnachie[5], R. J. Ellison[5], P. Flower[7], P. J. Flynn[4]
W. Galbraith[8], K. Heinloth[1], R. C. W. Henderson[4],
R. E. Hughes-Jones[5], J. S. Hutton[7], M. Ibbotson[5], H. P. Jakob[1],
M. Jung[1], B. R. Kumar[7], J. Laberrigue[6],
G. D. Lafferty[5], J. B. Lane[5], J. C. Lassalle[2], J. M. Levy[6],
V. Liebenau[1], R. H. McClatchey[8], D. Mercer[5], J. A. G. Morris[7],
J. V. Morris[7], D. Newton[4], C. Paterson[3], G. N. Patrick[7],
E. Paul[1], C. Raine[3], M. Reidenbach[1], H. Rotscheidt[1],
A. Schlosser[1], P. H. Sharp[7], I. O. Skillicorn[3],
K. M. Smith[3], K. M. Storr[2], R. J. Thompson[5],
Ch. de la Vaissiere[6], A. P. Waite[5], M. F. Worsell[5],
and T. P. Yiou[6]

ABSTRACT

A study of photoproduction of $K^+K^-\pi^+\pi^-$ shows a broad threshold enhancement, about 30% of which is due to $K^*K\pi$ production. This $K^*K\pi$ component shows no dynamical features indicative of the existence of a ϕ' vector meson in this channel.

(Submitted to Zeitschrift für Physik C)

There is considerable experimental uncertainty about the existence of ϕ' radial recurrences of the $\phi(1020)$ meson. Such states are expected to exist in the quark model analogous to the many known radial recurrences of the ψ and Υ. Potential models which accurately predict the masses of the ψ' and Υ' states [1] will not necessarily work well for mesons composed of light quarks. Potential models for light quarks [2,3] and models based on duality [4] do exist but their predictions often conflict with one another. In addition, non-perturbative techniques such as lattice QCD are not yet sufficiently refined.

The experimental situation is equally unclear. The radial recurrences of the low-mass vector mesons have been sought for some time at e^+e^- colliding beams and in diffractive photoproduction but to date only the $\rho'(1600)$ can be considered as a well-established resonance [5]; even here there is uncertainty about its true nature and about its width and partial decay modes. A $\rho'(1250)$ meson, required by some models, had been suggested by photoproduction data [6] but recent work has shown that the effect is probably due to B(1235) photoproduction [7]. Several ω' candidates have been reported from both e^+e^- annihilation and photoproduction but few of them have stood the test of time. At present there are two suggested ω' states. The first is a broad resonance (mass $\approx$ 1.6 GeV, width $\approx$ 0.5 GeV) decaying dominantly into $\omega\pi^+\pi^-$ indicated in a global fit to e^+e^- data [8], but not directly observed. The second is a narrower state (mass = 1.67 $\pm$ 0.02 GeV, width = 0.16 $\pm$ 0.02 GeV) seen in diffractive photoproduction of $\pi^+\pi^-\pi^0$ [9].

There are three ϕ' candidates currently in the literature. The first is the $\phi'(1680)$ seen mainly in $e^+e^- \to K^*K$ with a width of 0.18 GeV [8] but not seen at a corresponding rate in photoproduction [10]. The second is a peak with mass and width of 1.76 GeV and 0.08 GeV respectively, observed in two experiments in photoproduction of K^+K^- [11,12]. The third candidate is a broad enhancement in the mass spectrum of $K^*K\pi$, diffractively photoproduced [13]; this has mass ≈ 1.9 GeV and width ≈ 0.4 GeV.

It is the purpose of this letter to present an analysis of the reaction:

$$\gamma p \rightarrow K^+K^-\pi^+\pi^-p \qquad (1)$$

with improved statistical accuracy compared with Reference [13]. These new data favour the interpretation of the $K^*K\pi$ enhancement at a mass of 1.9 GeV as a non-resonant phenomenon rather than as a ϕ' candidate.

The data are from experiment WA57 at the CERN SPS. This experiment used a photon beam, tagged in the energy range 20-70 GeV, incident on a 60 cm long liquid hydrogen target situated within the magnetic field of the Omega Spectrometer. Secondary particles from interactions were measured by a system of MWPC's and drift chambers. A large-aperture threshold Cherenkov counter downstream of the spectrometer separated kaons from pions within the momentum range 5 to 17 GeV/c. A lead glass wall in combination with a photon position detector was used to detect photons from the interactions. A full description of the experiment can be found in Reference [14]. Offline geometrical reconstruction of the events in the spectrometer was performed by the program TRIDENT [15]. A second program evaluated the incident photon beam momentum, performed particle identification using the Cherenkov counter data and reconstructed γ-rays and π^0 mesons detected in the photon detector.

A total of 10^7 events were recorded, corresponding to a raw luminosity of 143 events nb^{-1}. The data for reaction (1) came from a trigger requiring 3 to 8 forward charged particles together with a signal indicating that at least one particle with momentum above 5 GeV/c gave no light in the threshold Cherenkov counter. A system of detectors in the median plane was used to veto events due to e^+e^- pair production. In the off-line data reduction, events were required to have 2 negative and 2 or 3 positive tracks; in the case of 3 positive tracks, one of them had to be kinematically consistent with being a recoil proton (19% of the final event sample were in this category). In addition, two tracks of opposite charge were required to give no light in the Cherenkov counter. Events having a signal in the photon detector were rejected. Finally, a well-reconstructed beam photon was required. For events surviving these selection criteria, the longitudinal momentum balance between the beam and the four-particle final state (ignoring the recoil-proton which would carry very little longitudinal momentum) was required to lie between -1 and +3.5 GeV/c. Because of well-understood inefficiencies in the Cherenkov counter [16,17], identification of tracks which failed to give light between the pion and kaon thresholds was ambiguous. In practice, each such track was assigned a probability, P, that the Cherenkov miss was genuine and was not due to inefficiency. Events were selected by the requirement that one kaon candidate had $P \geq 90\%$ and the other had $P \geq 50\%$. It has been checked that using a more stringent criterion (both kaon candidates had $P \geq 90\%$) caused no change to the physics conclusions [18]. Contamination of the data by $\bar{p}p\pi^+\pi^-$ events was found to be negligible by kinematic analysis of the events with an identified recoil proton. The missing mass squared to the $KK\pi\pi$ system for the selected events is given in Fig. 1 and shows a clear recoil proton peak. To select the final sample of 1118 events of reaction (1), the missing mass squared was required to be less than 2 GeV^2. The contamination of this sample from background from processes other than reaction (1) is estimated to be 35 ± 10%.

The K^+K^- mass spectrum, shown in Fig. 2, indicates production of $\phi\pi^+\pi^-$ states with a total cross section:

$$\sigma(\gamma p \to \phi\pi^+\pi^- p).B(\phi \to K^+K^-) = 18 \pm 7 \pm 6 \text{ nb}$$

(The errors are statistical and systematic respectively and the statistical error includes a contribution from the relatively large uncertainty in the background under the missing mass squared peak for the $\phi\pi\pi$ events). This result is consistent with the data of Reference [19]. The overall $\phi\pi^+\pi^-$ mass spectrum (not shown) is structureless. Since a $\phi' \to \phi\pi\pi$ decay would be OZI-violating one would not expect to observe any significant Φ' signal in this channel. For the subsequent analysis, events with a K^+K^- system in the mass range of the Φ-meson, 1.004 GeV to 1.036 GeV, were rejected leaving a final sample of 957 events.

Figure 3 gives the $K^{\pm}\pi^{\mp}$ mass spectrum for the final event sample and shows considerable $K^*(890)$ production. A study of the 2-dimensional plot of $K^+\pi^-$ mass versus $K^-\pi^+$ mass (not given) indicates that there is a negligible contribution from production of K^*K^* states and that there are equal fractions of $K^*\bar{K}\pi$ and $\bar{K}^*K\pi$ in the data. The curve on Fig. 3 shows a fit to the mass spectrum using a simple Breit-Wigner function to describe the peak and a parametrisation of the background (assumed incoherent) of the form:

$$f(m) = A(m - m_{th})^n \exp[-b(m - m_{th})]$$

where A, b and n are variable parameters and m_{th} is the $K\pi$ mass threshold. The fit gave mass and width of the K^* in agreement with the particle data tables and a peak area corresponding to 336 ± 22 $K^*K\pi$ events, 35% of the total sample.

The overall $K^+K^-\pi^+\pi^-$ mass spectrum is given in Fig. 4(a) and shows a broad enhancement rising from threshold to a peak at about 1.9 GeV, in agreement with the previous data of Reference [13]. In order to obtain distributions arising from the $K^*K\pi$ production, events were given a weight of +1 for each $K\pi$ combination in the K^* peak range (0.83 to 0.95 GeV), -1 for each combination in the wings regions (0.77 to 0.83 GeV and 0.95 to 1.01 GeV) and zero otherwise. Fig. 4(b) shows the $K^*K\pi$ mass distribution obtained in this way. The $K^+K^-\pi^+\pi^-$ mass distribution obtained by taking only events with a $K\pi$ combination in the K^* wings region (not shown) was found to be similar in shape to the $K^*K\pi$ spectrum of Fig. 4b indicating that the difference in width between the spectra of figures 4a and 4b is purely due to kinematics.

To investigate futher, Monte-Carlo events [20] were generated in such a way as to have many of the features of the observed events. The beam energy, E_γ, distribution was the same as the experimental one, the four-momentum transfer squared, t, from the beam to the $KK\pi\pi$ system was generated as exponentially distributed with a slope of 3.6 GeV^{-2} (c.f. 3.6 ∓ 0.2 GeV^{-2} for the real data) and the total production cross section was assumed constant as a function of $E\gamma$ since only a weak dependence would be expected for diffractive dissociation (in fact, for the data, the cross section fell as $E\gamma^{-0.17\pm0.14}$ consistent with this expectation). The overall $KK\pi\pi$ mass distribution was generated to agree with Fig. 4(a) and the relative contributions from K^* and non-K^* events were set to the values obtained from the fit to the $K\pi$ mass spectrum (Fig. 3). All the decay angular distributions were according to phase space.

The Monte-Carlo events were passed through a simulation of the apparatus and were subjected to exactly the same analysis procedures as the real data. The curve on Fig. 4(b) shows the resulting simulated $K^*K\pi$ mass spectrum. The agreement between the data and the curve shows that the overall shape of the $K^*K\pi$ mass spectrum follows directly from the $KK\pi\pi$ mass spectrum and kinematics, and there is no need for dynamical effects.

The decay angular distributions of the $K^*K\pi$ system were investigated in the s-channel helicity frame. If a significant fraction of the events were due to diffractive production of a Φ' state then s-channel helicity conservation (SCHC) could hold in the production [21,5,22]. Assuming that such a Φ' decays to $K^*K\pi$ in relative s-waves, the distribution of the K^* direction in the $K^*K\pi$ system would be isotropic while the K-direction in the K^* frame would follow a $\sin^2\Theta$ distribution; here, Θ is the polar angle between the particle direction and the helicity axis. The previous study [13] of reaction (1) was unable to distinguish between isotropy and $\sin^2\Theta$ for this latter distribution. The results of the present experiment are shown in Figs. 5(a) and 5(b) for the two distributions described above. The solid curve on both figures is the expectation for isotropic decay distributions corrected for the experimental acceptance. It is clear that both distributions are in good agreement with the assumption of isotropy. Production of a Φ'-meson by SCHC would give a $\sin^2\theta$ distribution in Fig. 5(b), the K-direction from the K^* in the K^* rest system relative to the helicity axis; the acceptance-corrected $\sin^2\theta$ distribution is shown as the dashed curve. The data are in better agreement with the solid curve ($x = 8.6$ for 8 data points) than with the dashed curve ($x^2 = 23.3$) and so favour the assumption of isotropy rather than the production of a vector meson by an s-channel helicity conserving mechanism.

The production cross-sections were evaluated using the acceptance figures obtained from the simulation. Correction factors were applied to account for secondary particle interactions within the hydrogen target and possible decay of $K^{\pm}$-mesons before reaching the Cherenkov counter. The results were:

$$\sigma(\gamma p \rightarrow K^+K^-\pi^+\pi^-p) = 136 \pm 4 \pm 42 \text{ nb}$$

of which

$$\sigma(\gamma p \rightarrow K^*K\pi p) = 48 \pm 4 \pm 15 \text{ nb}$$

in agreement with the previous study [13] of reaction (1). These results are for the complete observable $KK\pi\pi$ mass range.

In conclusion, there is no evidence in diffractive photoproduction of $K^*K\pi$ for the existence of a Φ' vector meson, a radial recurrence of the $\Phi(1020)$. The data do not rule out such a state but there appear to be no dynamical features of the data which require explanation in terms of a Φ' meson.

We are grateful to the Omega group at CERN for their help in running the spectrometer and providing on-line and off-line software. The work of the technical support staff in our home institutions, and the support at the computer centres at the Rutherford Appleton Laboratory, CERN and the RHRZ at Bonn have been invaluable. We thank the SERC (UK), the BMFT (Fed. Rep. Germany) and the IN2P3 (France) for financial support.

References

1. See, for example, E. Eichten et al., Phys. Rev. D17 (1978) 3090 and D21 (1980) 313(E).
2. H. J. Schnitzer, Phys. Rev. 18 (1978) 3482.
3. N. Isgur, XVI Rencontre de Moriond, 1981.
4. A. J. Hey and D. Morgan, Rep. Progr. Phys. 41 (1978) 657.
5. D. Aston et al., N. Phys. B189 (1981) 15 and references therein.
6. D. Aston et al., Phys. Lett. 92B (1980) 211.
7. M. Atkinson et al., N. Phys. B243 (1984) 1.
8. J. Buon et al., Phys. Lett. 118B (1982) 221.
9. M. Atkinson et al., Phys. Lett. 127B (1983) 132.
10. M. Atkinson et al., N. Phys. B231 (1984) 1.
11. D. Aston et al., Phys. Lett. 104B (1981) 231.
12. M. Atkinson et al., Z. Phys. C27 (1985) 233.
13. D. Aston et al., Phys. Lett. 92B (1980) 219.
14. D. Aston et al., N. Phys. B231 (1984) 15.
15. J. C. Lassalle, F. Carena and S. Pensotti, Nucl. Instr. Meth. 176 (1980) 371.
16. T. J. Axon, Thesis, University of Manchester, 1984.
17. M. Reidenbach, Bonn IR-82-1.
18. A. Schlösser, Bonn IR-84-15.
19. M. Goodman et al., Phys. Rev. D22 (1980) 537.
20. J. Friedman, SAGE Reference Manual, SLAC Computation Group. Technical Memo 145 (1972).
21. T. H. Bauer et al., Rev. Mod. Phys. 50, No. 2 (1978) 261.
22. M. Atkinson et al., Z. Phys. C26 (1985) 499.

Figure Captions

Figure 1

Missing mass squared to $K^+K^-\pi^+\pi^-$

Figure 2

Mass spectrum of K^+K^-

Figure 3

Mass spectrum of $K^\pm\pi^\mp$. The curve is from a fit described in the text.

Figure 4

(a) $K^+K^-\pi^+\pi^-$ mass spectrum

(b) $K^*K\pi$ mass spectrum obtained as described in the text. The curve is from a Monte-Carlo simulation (see text).

Figure 5

(a) Polar decay angular distribution of K^* in $K^*K\pi$ rest frame relative to the helicity axis. The solid curve represents an isotropic distribution modified by acceptance.

(b) Angular distribution of K from K^* decay in K^* rest frame relative to helicity axis. The solid curve shows an isotropic distribution and the dashed one represents a $\sin^2\theta$ dependence, both corrected for acceptance.

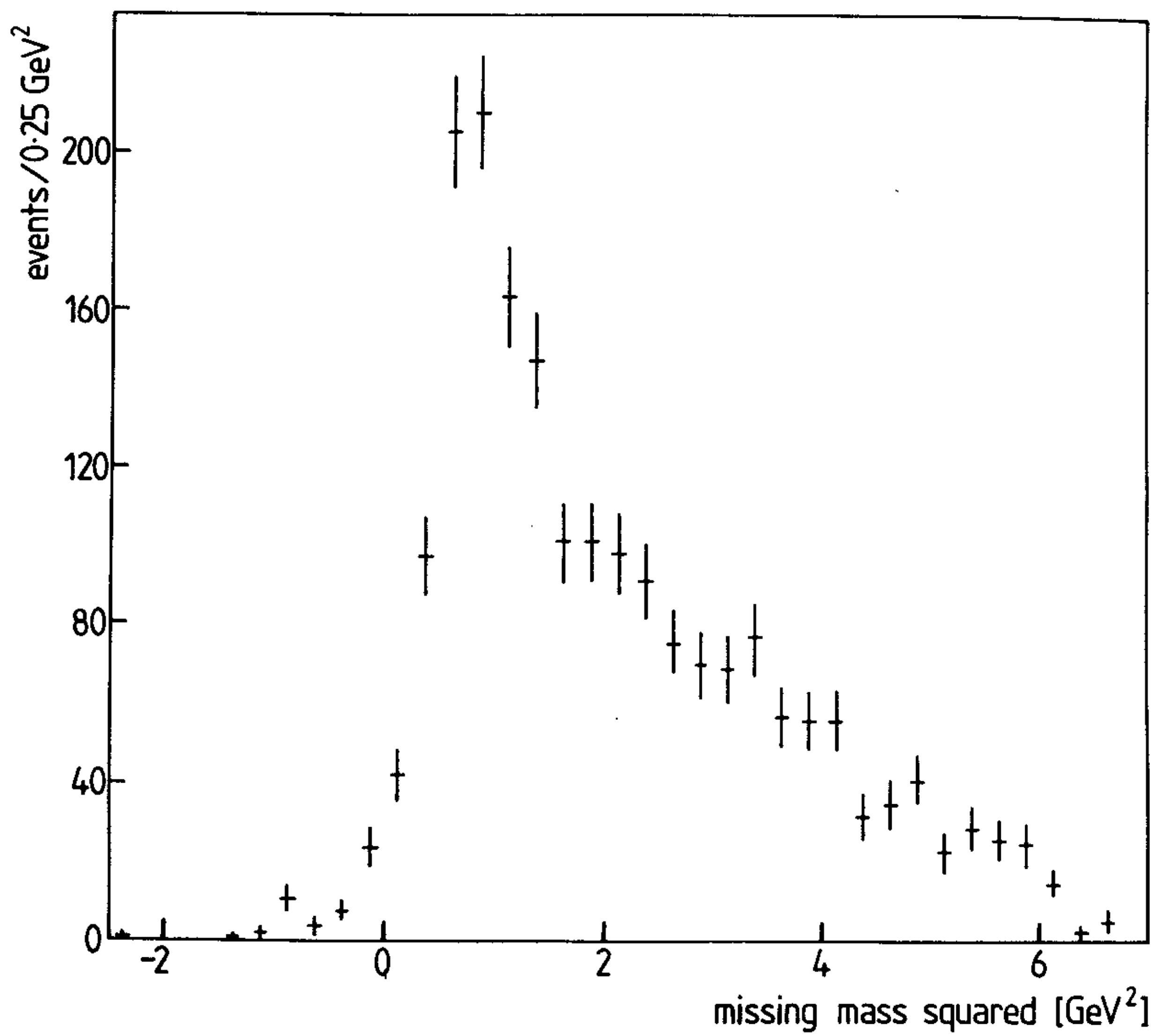
events/0·25 GeV²
200
160
120
80
40
0
-2
0
2
4
6
missing mass squared [GeV²]

Fig. 1

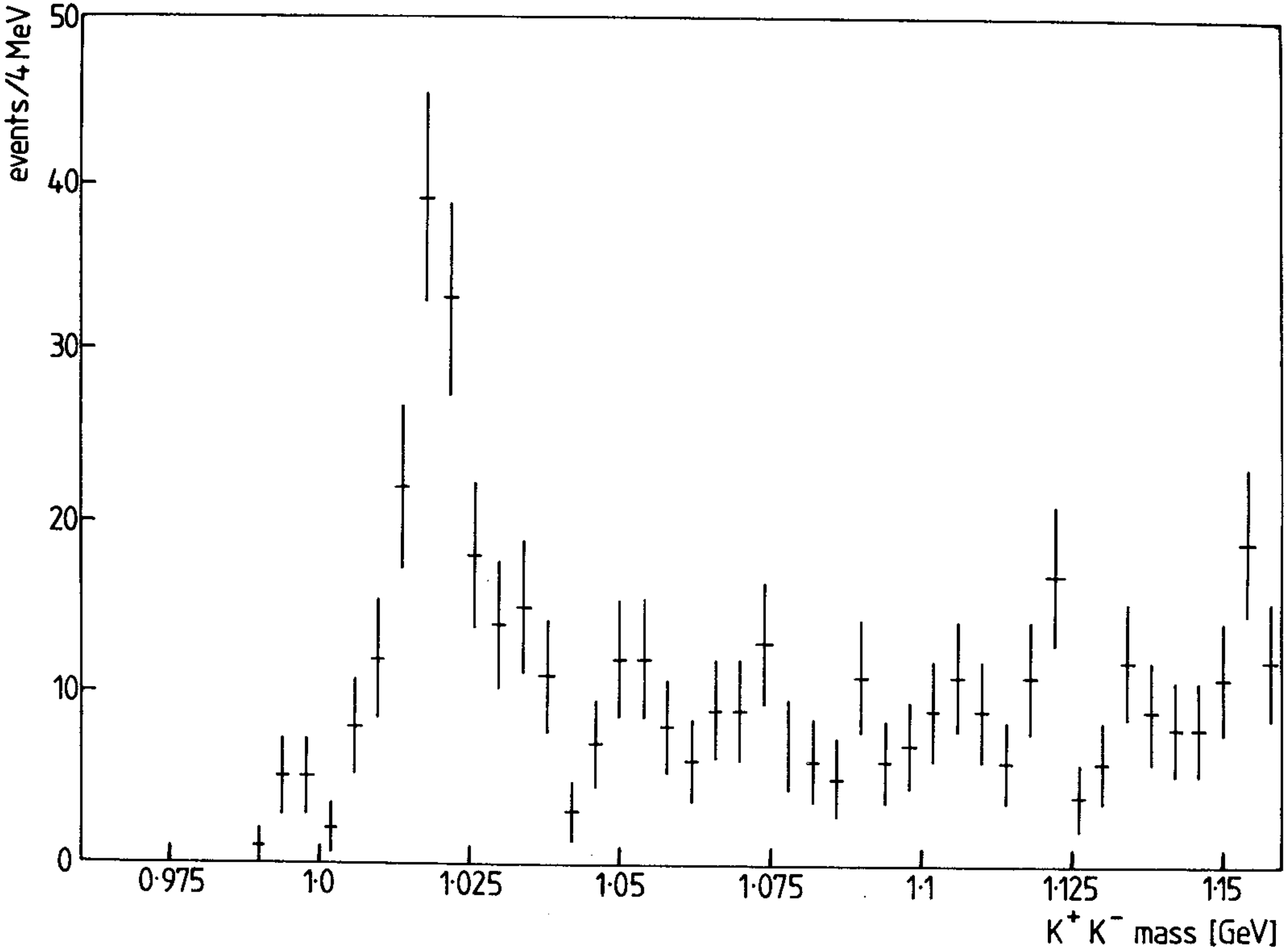
events/4 MeV
50
40
30
20
10
0
0·975
1·0
1·025
1·05
1·075
1·1
1·125
1·15
K⁺ K⁻ mass [GeV]

Fig. 2

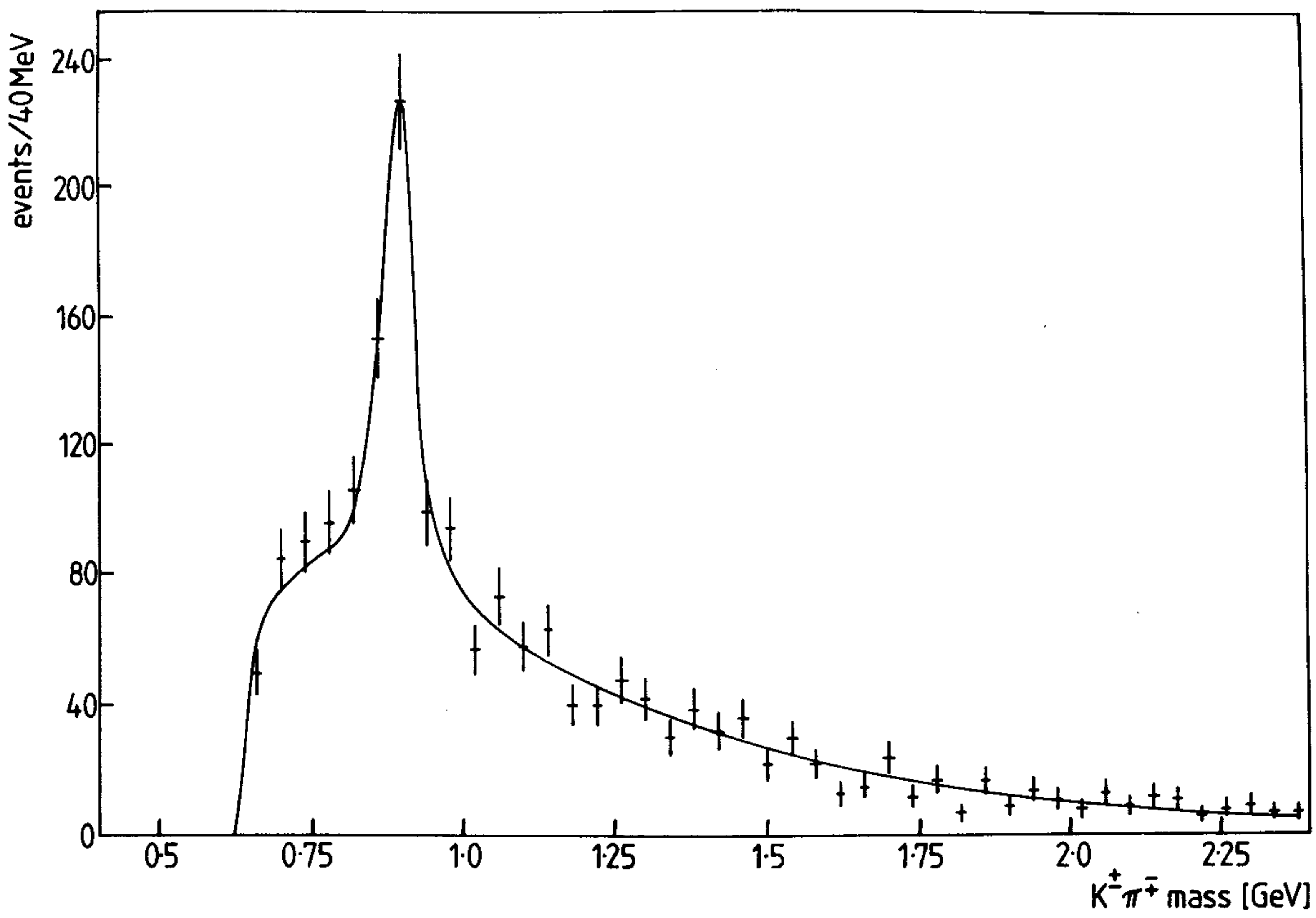
events/40MeV
240
200
160
120
80
40
0
0·5
0·75
1·0
1·25
1·5
1·75
2·0
2·25
K$^{\pm}\pi^{\mp}$ mass [GeV]

Fig. 3

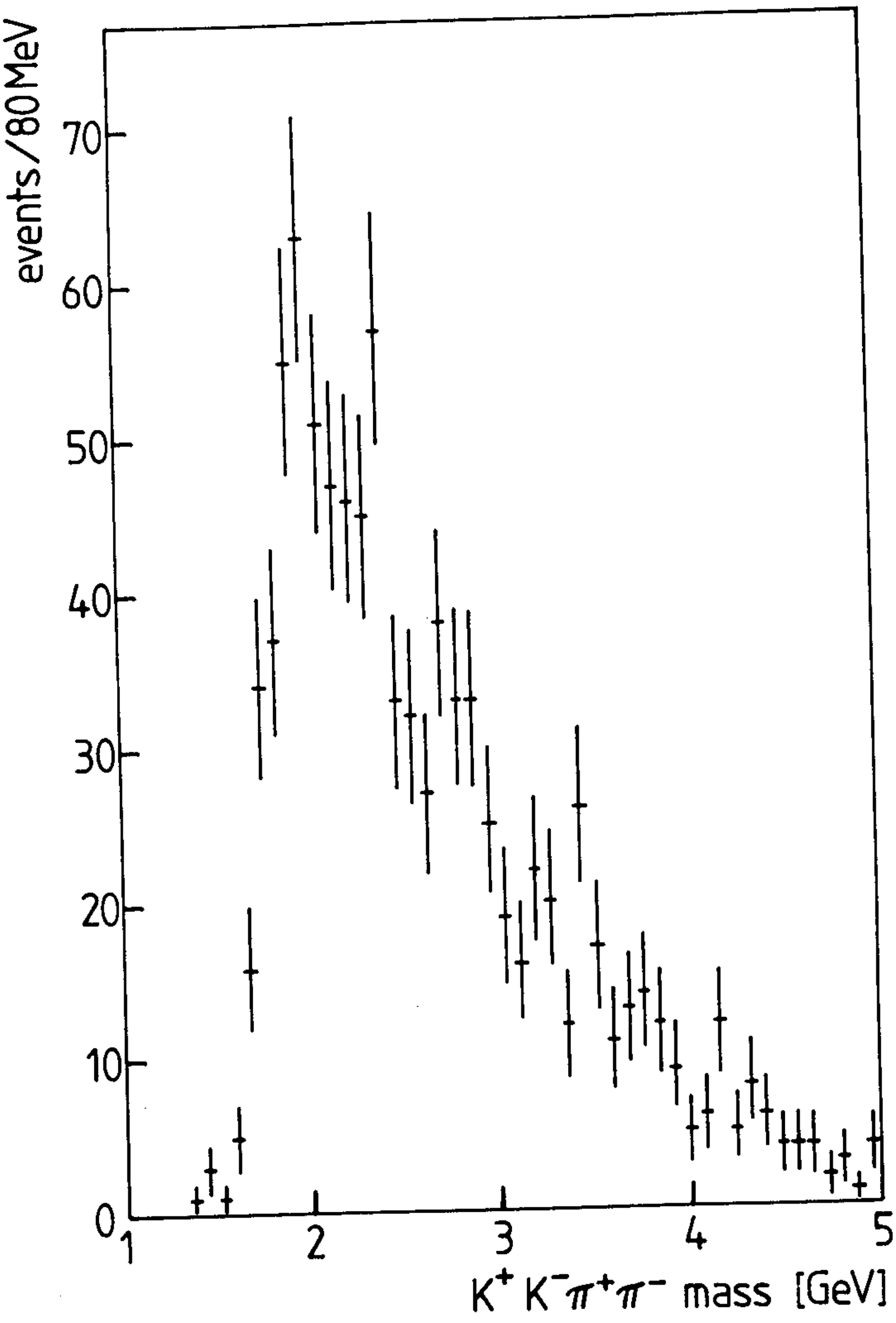

Fig. 4a

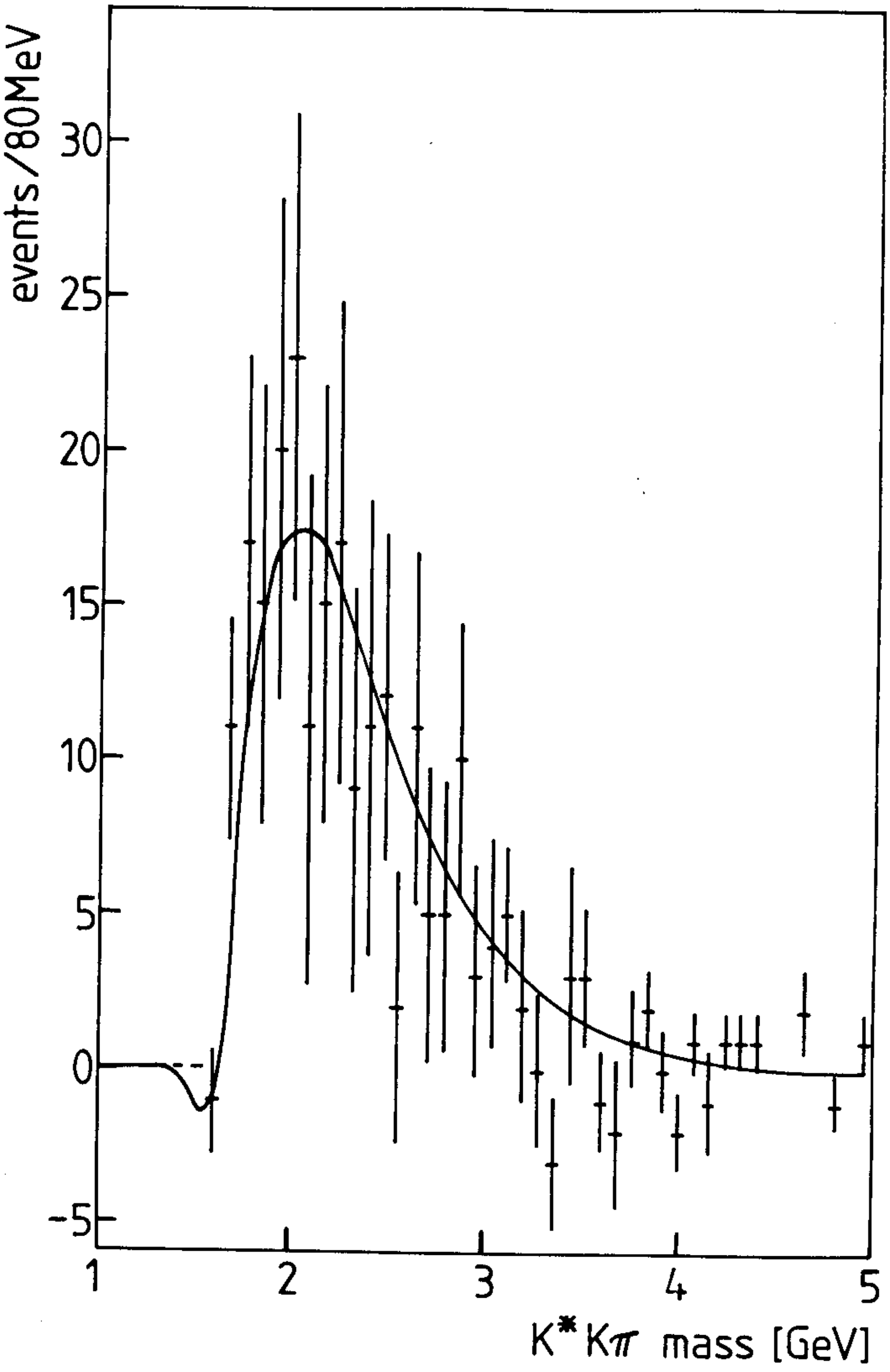

Fig. 4b

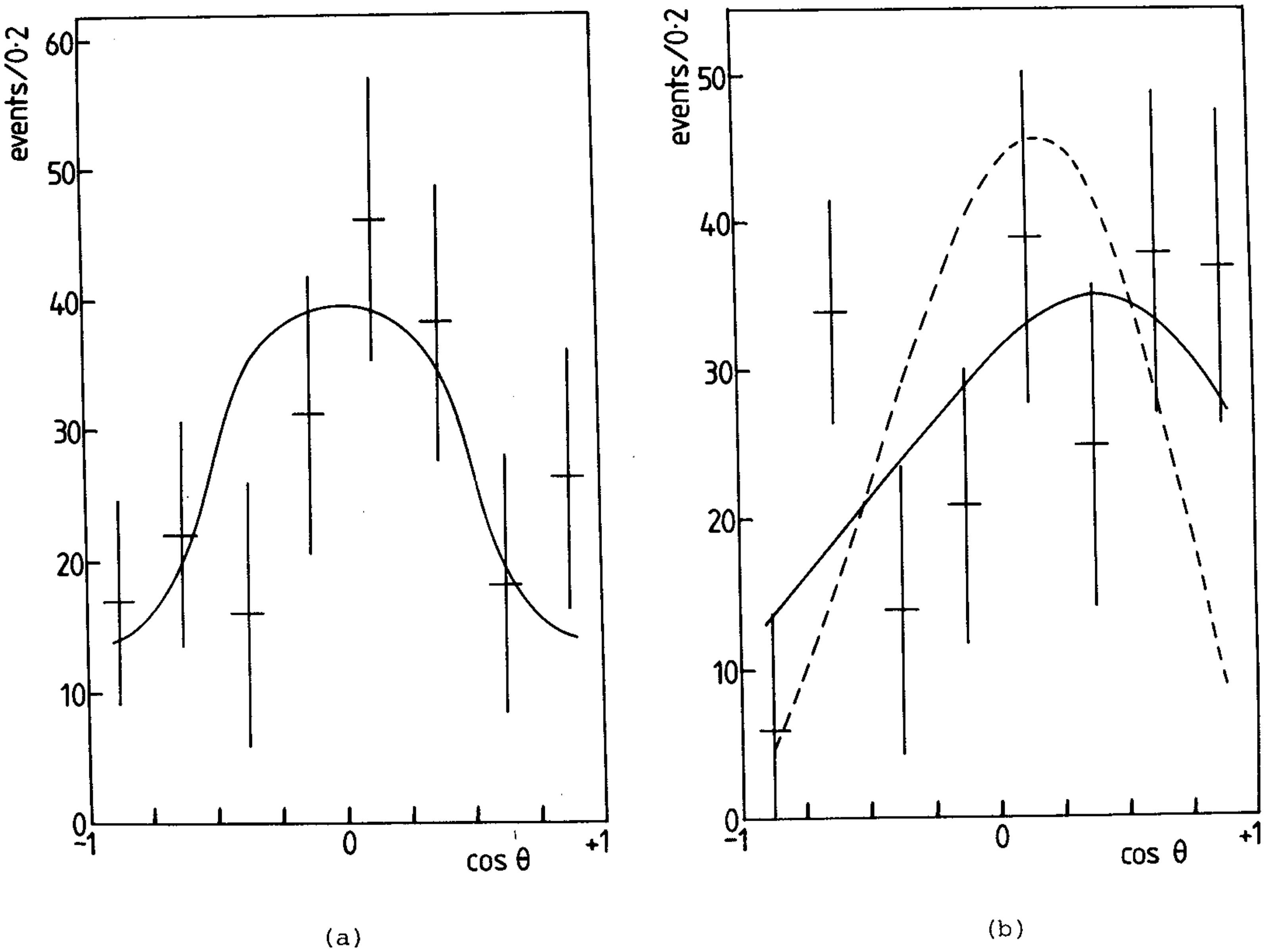
events/0·2
60
50
40
30
20
10
0
-1
0
+1
cos θ
(a)
events/0·2
50
40
30
20
10
0
-1
0
+1
cos θ
(b)

Fig. 5